Lab on a Chip

Cite this: *Lab Chip*, 2012, **12**, 4864–4869

www.rsc.org/loc

PAPER

Visual and high-throughput detection of cancer cells using a graphene oxide-based FRET aptasensing microfluidic chip†

Lili Cao, Liwei Cheng, Zhengyong Zhang, Yi Wang, Xianxia Zhang, Hui Chen, Baohong Liu, Song Zhang* and Jilie Kong*

Received 16th May 2012, Accepted 5th September 2012
DOI: 10.1039/c2lc40564d

Rapid and efficient measurement of cancer cells is a major challenge in early cancer diagnosis. In the present study, a miniature multiplex chip was created for *in situ* detection of cancer cells by implementing a novel graphene oxide (GO)-based Förster resonance energy transfer (FRET) biosensor strategy, *i.e.* assaying the cell-induced fluorescence recovery from the dye-labeled aptamer/graphene oxide complex. Fluorescence intensity measurement and image analyses demonstrated that this microfluidic biosensing method exhibited rapid, selective and sensitive fluorescence responses to the quantities of the target cancer cells, CCRF-CEM cells. Seven different cancer cell samples can be measured at the same time in such a microfluidic chip. The linear response for target CCRF-CEM cells in a concentration range from 2.5×10^1 to 2.5×10^4 cells mL^{-1} was obtained, with a detection limit about 25 cells mL^{-1}, which is about ten times lower than those of normal biosensors. The novel fluorescence biosensing microfluidic chip supplies a rapid, visible and high-throughput approach for early cancer diagnosis with high sensitivity and specificity.

Introduction

Development of a detection method for cancer cells at their earliest stages is a key challenge in cancer diagnostics. As the malignant cells are normally present at low concentrations in blood, traditional analytical techniques, such as flow cytometry based on immunophenotypic analysis[1] and PCR-based DNA analysis,[2] do not meet the requirements of point-of-care (POC) diagnostics as they require expensive instruments, long analytical times and are complicated to operate.[3] In contrast, microfluidic devices are promising platforms that can be used to create inexpensive and fast approaches for cell purification and detection due to their small physical dimensions and high-throughput.[4–7] For example, many microfluidic devices with different working principles, such as cell-affinity micro-chromatography,[4,5] magnetic activated cell sorting,[6] and cellular biophysics (*e.g.* cell size, adhesion, deformability, and dielectrophoresis),[7] have been developed to purify and detect rare cancer cells. Notably, compared with the limited availability for highly selective antibodies in capturing targeted cancer cells, aptamers, artificial oligonucleotides originated from *in vitro* SELEX, have shown high affinity, specificity and stability in particular,[8–10] and have been employed as ideal recognizing elements in microfluidic chips for cancer cell analysis. Phillips *et al.*[5] reported a microfluidic device modified with aptamers to enrich rare cancer cells, which specifically captured target cells (>97% purity) with a high efficiency (>80%). Although this aptamer-based microfluidic device provides an effective approach for enriching rare cancer cells, the *in situ* detection of cancer cells in such a microfluidic chip is still a challenge. Thus, it is necessary to develop a simple aptasensing microfluidic chip for the sensitive, visual and high-throughput detection of cancer cells in early cancer diagnosis.

However, the direct detection of cancer cells by the aptamer-based microfluidic chip is severely hindered by the fact that most aptamer–cell interactions do not produce an easily measureable output. To solve this problem, the primary cell-detecting strategy is designing an 'always-on' aptamer probe with sensitive tag molecules, such as magnetic,[11] colorimetric[12] and fluorescent agents,[10,13] in which the reporter-labeled aptamer probes will specifically bind to the target cells and produce obviously enhanced signals. But the implementation of these sensitive aptasensing techniques with a high-throughput microfluidic chip is quite difficult because complex washing steps were normally needed to improve the signal-to-background ratio for immobilized aptamers. Recently, a more efficient 'signal-on' aptasensing strategy based on Förster resonance energy transfer (FRET) has attracted more attention for visualizing cancer cells. Shi *et al.*[14] reported a double-labeled FRET aptamer probe for *in vivo* cancer cell imaging, which underwent a conformational alteration along with an activated fluorescence upon binding to targeted cancer cells. Considering FRET has an inherently high sensitivity,[15–17] and exhibits good compatibility with microfluidic

Department of Chemistry, Fudan University, Shanghai 200433, P. R. China. E-mail: songzhang@fudan.edu.cn; jlkong@fudan.edu.cn; Fax: +86 21 65641740; Tel: +86 21 65642405
† Electronic supplementary information (ESI) available. See DOI: 10.1039/c2lc40564d

devices[18] and homogeneous detections,[19,20] the implementation of FRET on biosensing microfluidic chips for detecting cancer cells is an ideal choice and aptamer immobilization and washing steps might be eliminated. However, up to now, there have no reports about using the FRET aptasensing microfluidic chips in directly detecting cancer cells. Possible reasons might be the complicated and rational design of DNA sequences, the difficult and compulsory modification of a pair of fluorophores and quenchers simultaneously, and the low efficiency of FRET.[21]

Coupling nanomaterials with biomolecular recognition events represents a new direction toward the development of novel molecular diagnostic tools.[22,23] Graphene oxide (GO), a two-dimensional carbon crystal with only one atom thickness, has attracted much attention due to its excellent optical and electrical properties and showed great importance in nanoelectronics,[24] sensors,[25] nanocomposites,[26] and fluorescence quenching.[23,27] Meanwhile, GO can differentiate various DNA structures (*e.g.* ssDNA, dsDNA and stem-loop) due to the distinct interactions between them. By combining the super quenching capacity with the unique ability for DNA adsorbtion by GO, a lot of highly sensitive FRET aptasensors have been exploited for homogenous detection of biomolecules such as DNA,[22,27] petides,[28] and proteins.[29] However, exploration of GO for living cells analysis and *in situ* monitoring still remains at a very early stage.

Herein, we first demonstrate a multiplex microfluidic chip integrated with the GO-based FRET strategy to create a screening assay for tumor cells. The analytical efficiency of the microfluidic chip for *in situ* detection of target cancer cells is found to be highly improved, and microliters of multi-samples can be analyzed at the same time with a microscopy system in a high-throughput manner. The simple, selective, and miniaturized chip shows great potential in developing a rapid diagnostic assay for cancer cells.

Experimental section

Materials

Fluorophore carboxy fluorescein (FAM)-labeled aptamer oligonucleotides with a sequence of 5′-FAM-ATC TAA CTG CTG CGC CGC CGG GAA AAT ACT GTA CGG TTA GAT-3′ (FAM-Sgc8) and 5′-FAM-CAC CGG GAG GAT AGT TCG GTG GCT GTT CAG GGT CTC CTC CCG GTG-3′ (as the control, FAM-TD05) were obtained from Sangon Corp. Shanghai. Graphite powders were obtained from Sinopharm Chemical Reagent Co., Ltd (China). Other reagents were purchased from Shanghai Chemical Reagent Co., Ltd. All chemicals were of analytical purity and were used as received without further purification. Deionized water was used for all experiments.

Cells

T-cell acute lymphoblastic leukemia cells (CCRF-CEM cells), B-cell lymphoma lines (Raji cells), human cervix cancer cells (HeLa cells), human breast adenocarcinoma cell (MCF-7 cells), and human non-small-cell lung cancer line (NCIH1650 cells) were purchased from Cell Bank of Chinese Academy of Sciences. CCRF-CEM and Raji cells were cultured in RPMI 1640 medium supplemented with 10% fetal bovine serum (FBS) and 100 units/mL penicillin streptomycin and incubated at 37 °C in a humidified incubator containing 5% wt/vol CO_2. HeLa cells, MCF-7 cells and NCIH1650 cells were cultured in DMEM medium supplemented with 10% FBS. The cell density was determined using a hemocytometer, and this was performed prior to any experiments.

Apparatus

Fluorescence spectra were recorded on a Cary Eclipse spectrophotometer (Agilent Co., USA) with an excitation wavelength at 488 nm. The cell images were recorded on a TCS SP5 confocal microscopy system (Leica Co., Germany) with a tunable argon ion laser (458, 488, 514 nm) and a separate photomultiplier tube for scanning. Flow cytometric analysis was performed on FACS caliber flow cytometer (Becton Dickinson, USA). Atomic force microscopy (AFM) images were measured using a Nanoscope Multimode IV atomic force microscope (Vecco precise instrument corp., USA) in tapping mode.

Microfluidic chip design and fabrication

Microfluidic channel patterns and the corresponding master were designed and fabricated by mechanical microfabrication. A PDMS replica was produced by molding as described previously by our lab.[30,31] In brief, Sylgard 184 PDMS precursor was mixed thoroughly with its cross-linking catalyst at 10 : 1 (w/w) and degassed by vacuum for 30 min. The precursor mixture was cast against the silicon mold and polymerized at 90 °C for 1 h. Then the cured PDMS replica was gently peeled from the master, and the columnar inlet and outlet were manually drilled for each multichannel, and irreversibly sealed against a clean microscope cover glass by a treatment with oxygen plasma for 5 min to form a leak-proof microchip. The PDMS chip had 33 uniform microchannels with a width and depth of 100 μm (as shown in Fig. 1A). All the liquids were pumped into the microfluidic chip *via* poly(ethylene) tubing and multichannel syringe pumps (Longer Apparatus, Shanghai).

Synthesis and characterization of GO

Graphene oxide (GO) nanosheets were prepared from the exfoliated graphite oxide by using modification of a literature procedure.[23] Briefly, graphite oxide was prepared from graphite powder by Hummers method,[32] and dissolved in deionized water at certain concentration and exfoliated by sonication for 30 min to ensure most graphite oxide was exfoliated to single-layer GO nanosheets. The unexfoliated graphite oxide was removed by centrifugation at 10 000 rpm for 5 min. The brown suspension obtained was the solution of GO nanosheets with a concentration about 1.0 mg mL^{-1}. The as-prepared GO nanosheet samples were characterized with AFM, TEM, XRD, FT-IR and Raman Spectroscopy. And AFM images (Fig. S1A, ESI†) show that the thickness of GO was about 0.7 ± 0.2 nm, indicating its single-layer. The TEM image of GO (Fig. S1B†) shows that the nanosheet was extremely thin and highly transparent.

An integrated microfluidic chip for assaying cancer cells

To perform the high-throughput assay for CCRF-CEM cells, the aptasensing microfluidic chip applied a 'premixing and detecting'

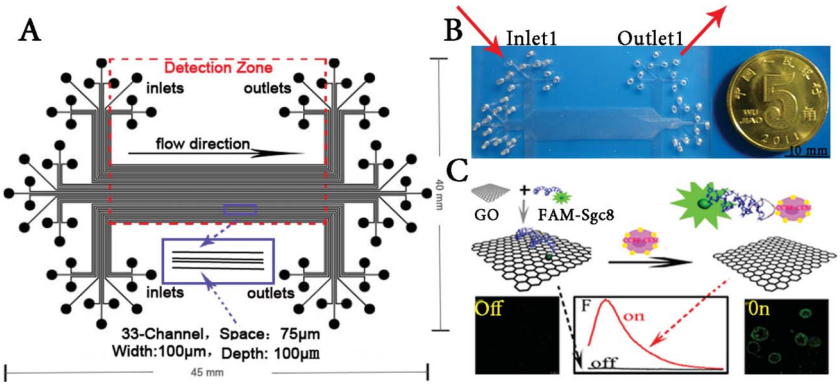

Fig. 1 (A) Schematic setup and (B) the photograph of the GO-based FRET aptasensing microfluidic chip. Scale bar: 10 mm. (C) The principle of a 'signal-on' aptasensor for detecting CCRF-CEM cells by assaying the cell-induced fluorescence recovery of GO/FAM-Sgc8

strategy.[27,29] In brief, the FRET probe of GO/FAM-Sgc8 was prepared by premixing FAM-Sgc8 (25 nM) and GO dispersion (6.0 μg mL^{-1}) in a 10 mM PBS buffer (pH 7.4, containing 137 mM NaCl, 2.7 mM KCl) for 5 min to completely quench the fluorescence. Then, each PDMS microchannel was first piped with a kind of cell-mixture sample (40 μL), which contained the GO/FAM-Sgc8 and serial dilutions (10-fold) of CCRF-CEM cells ranging from 2.5×10^1 to 2.5×10^6 cells mL^{-1}. The microfluidic chip was then incubated for 20 min at 37 °C in a humidified incubator (containing 5% wt/vol CO_2) for 20 min to ensure efficient interaction between FAM-Sgc8 and CCRF-CEM cells, leading to the recovery of the quenched fluorescence. Finally, the microfluidic chip (in a static system) was subjected to analysis with a confocal fluorescent microscope at 10× objective and a scan speed of 200 Hz, and different cell mixture samples in 7 microchannels were analyzed simultaneously. Also, to study the specificity of the microfluidic assay, different cancer cell samples, such as Raji cells, MCF-7 cells, HeLa cells and NCIH1650 cells, were incubated with GO/FAM-Sgc8 in the same process and their fluorescent intensities were recorded, respectively.

In order to further confirm specific interactions between FAM-Sgc8 and CCRF-CEM cells, flow cytometry and confocal fluorescent microscopy were performed to detect different aptamer–cell systems, *e.g.* FAM-Sgc8 and CCRF-CEM cells, FAM-TD05 (as the control probe) and CCRF-CEM cells, and FAM-Sgc8 and HeLa cells (as the control cell). Before flow cytometry and fluorescent imaging analysis, the cell mixtures were centrifuged at 1000 rpm for 5 min, washed with 10 mM PBS buffer twice, and then re-dispersed in 500 μL of PBS buffer.

Cytotoxicity assay

In vitro cytotoxicity of GO was evaluated by performing cell counting kit-8 (CCK-8) assays with CCRF-CEM cells. Cells were incubated with 10% fetal bovine serum supplemented with RPMI 1640 medium at 37 °C, in a humidified atmosphere of 5% CO_2. 100 μL cell suspensions were added into a 96-well cell culture plate (1.0×10^5 cells/well), and then 100 μL GO (10, 20, 40, 100, 200, 300 μg mL^{-1}) was added and the plates were incubated for 24 h. In order to avoid the possible influence of GO on the CCK-8 assay, the 96-well plate was taken out and centrifuged for 5 min. The suspensions were pipetted off and 200 μL new RPMI 1640 medium was added, and then a 10 μL CCK-8 solution was added to each well and incubated for another 2 h. The assays were performed according to the manufacturer's instructions. The absorbance of Formazan at 450 nm was measured by a scanning multiwall spectrometer (SPR-960, Sunostik).

Results and discussions

Microfluidic device and detection principle

Developing an integrated, sensitive and high-throughput assay for the detection of cancer cells is challenging. For this purpose, a 33-channel microfluidic chip integrated with the GO-based FRET aptasensor was designed and employed to detect target CCRF-CEM cells with a confocal fluorescence scanning microscope (Fig. 1). The microfluidic chip was made with PDMS materials by soft lithography,[29,30] and the general design and dimensions of the device is illustrated in Fig. 1A. Since the FRET worked as a homogeneous assay,[18–20] the aptamer immobilization and washing steps were no longer needed in the microfluidic chip. A parallel-mode multichannel was adopted for integrating multiplex FRET biosensors into the microfluidic chip, allowing a high-throughput assay of different cell samples simultaneously. The fabricated PDMS-microfluidic chip was 5.0 cm × 4.5 cm (in Fig. 1B) and each parallel microchannel had a width and depth of 100 μm. In order to achieve on-chip detection (Fig. 1C), a single fluorophore-labeled aptamer (FAM-Sgc8) was chosen as a model of the 'signal-on' molecular probes because of its high affinity for CCRF-CEM cells.[10] In the free state, the FRET probe of GO/FAM-Sgc8 exhibited a quenched fluorescence because of π–π stacking interactions between FAM-Sgc8 and GO, whereas once target cells were introduced, the interaction between FAM-Sgc8 and CCRF-CEM cells was strong enough to release FAM-Sgc8 from GO, and then the fluorescence was recovered. Thus, *in situ* detection of target cancer cells in the microfluidic chip was achieved.

FRET of GO/FAM-Sgc8 in the integrated microfluidic chip

The fluorescence quenching capacity of the GO/FAM-Sgc8 probe in such an integrated microfluidic chip was first evaluated by a confocal fluorescence scanning microscope. From the scanning image of the 8 microchannels (Fig. 2A), it shows that

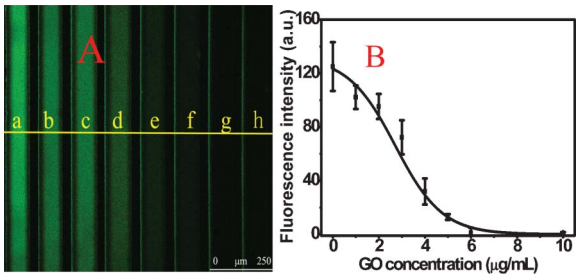

Fig. 2 (A) Fluorescence quenching micrograph of different GO/FAM-Sgc8 in an integrated microfluidic chip. (B) The relationship between fluorescence intensity and the concentration of GO. FAM-Sgc8 concentration: 25 nM. Excitation wavelength: 488 nm. Scale bar: 250 μm.

the fluorescence of GO/FAM-Sgc8 was quenched promptly, and the fluorescence intensity (at 520 nm) remarkably decreased with the increased concentration of GO. When the concentration of GO reached 6.0 μg mL^{-1}, over 98% of fluorescence was quenched in 2 min (Fig. S2, ESI†). Here, the ratio of fluorescence quenching was calculated by $(F_i\text{-}F_q)/F_i$, and F_i and F_q were fluorescent intensities before and after the quenching process, respectively. Notably, compared with the normal FRET probes needing modification of the fluorophore and a quencher simultaneously, the GO/FAM-Sgc8 had a simplified design by using the single-labeled FAM-Sgc8 (a commercially available aptamer). Moreover, the quenching efficiency in our study was higher than that in other cases, for example, 80% fluorescence quenched by SDS-graphene for thrombin detection[29] and 97% fluorescence quenched by GO for HIV1 analysis.[27] The higher quenching efficiency in the present study can be ascribed to the strong adsorption of FAM-Sgc8 on GO through π–π stacking and the high-efficiency of GO as a nanoquencher of the FRET probe. Considering that it is important to quench the fluorescence completely to obtain a low background signal, we extended the incubation time to 5 min for preparing the effective FRET probe of GO/FAM-Sgc8 in the following experiment.

Cell-induced fluorescence recovery of GO/FAM-Sgc8

As shown in Fig. 1C, it is hypothesized that the introduction of CCRF-CEM cells will induce the fluorescence recovery of GO/FAM-Sgc8 because of the strong interaction between aptamers and cells. To prove this hypothesis, different samples with GO/

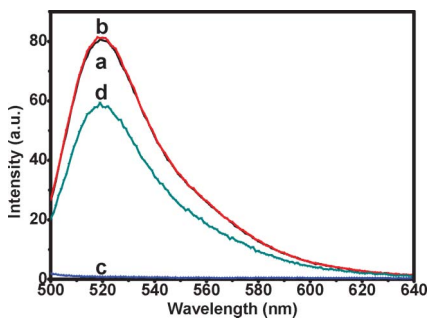

Fig. 3 CCRF-CEM cell-induced fluorescence recovery of GO/FAM-Sgc8. Fluorescence spectra of (a) FAM-Sgc8, (b) FAM-Sgc8+cell, (c) FAM-Sgc8+GO, (d) FAM-Sgc8+GO+cell. CCRF-CEM cells concentration: 2.5 × 10^6 cells mL^{-1}. Other conditions were as in Fig. 2.

FAM-Sgc8 and CCRF-CEM cells were first studied by quantitative fluorescence measurements. When we added the GO/FAM-Sgc8 into the CCRF-CEM cells, the quenched fluorescence of GO/FAM-Sgc8 (Fig. 3c) was switched on, and about 55% of the initial fluorescence intensity was observed to be recovered (Fig. 3d). While in the absence of GO, no obvious change in fluorescent intensity for FAM-Sgc8 and CCRF-CEM cells (Fig. 3b) was observed, indicating that the CCRF-CEM cells had little influence on the fluorescence of free FAM-Sgc8. These results imply that, in its free state, FAM-Sgc8 (as a ssDNA aptamer) easily bonds to GO through π–π stacking interactions between DNA bases and GO, and the fluorescence is quenched through FRET. However, when target CCRF-CEM cells are added into the GO/FAM-Sgc8 solution, the specific binding between target cells and aptamers is strong enough to change the free folding of ssDNA into a stable hairpin structure,[14] and then the FAM-Sgc8 probe is released from GO and the quenched fluorescence of GO/FAM-Sgc8 is recovered as shown in Fig. 1C.

In order to further confirm that the fluorescence recovery was triggered by the specific interaction between FAM-Sgc8 and CCRF-CEM cells, flow cytometry and confocal fluorescence microscopy were performed. As shown in Fig. 4A, the flow cytometric assays demonstrate that CCRF-CEM cells emitted increased fluorescence intensity when they were incubated with the FAM-Sgc8 probe than with the control FAM-TD05 probe, reflecting the fact that FAM-Sgc8 probe selectively binds with CCRF-CEM cells. The fluorescence and transmission images of CCRF-CEM cells incubated with GO/FAM-Sgc8 and GO/FAM-TD05 (Fig. 4B) also prove that the specific interaction between FAM-Sgc8 and CCRF-CEM cells causes the fluorescence recovery of the GO/FAM-Sgc8 biosensor. A significant fluorescence signal is observed at the surface of CCRF-CEM cells in the presence of GO/FAM-Sgc8, suggesting that it is the specific binding between FAM-Sgc8 and CCRF-CEM cells initiating the fluorescence recovery, which is consistent with the previous report[10] that the Sgc8 probe can interact with the cell membrane protein tyrosine kinase-7 (PTK7), a protein closely associated with a number of cancers. In contrast, there is no observable fluorescence signal for the GO/FAM-TD05 and CCRF-CEM cells, implying that the random FAM-TD05 probe

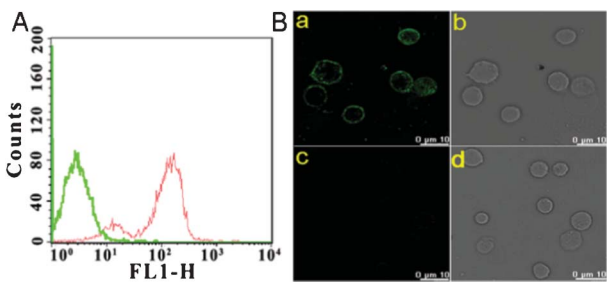

Fig. 4 Selectivity binding of aptamers to CCRF-CEM cells. (A) Flow cytometry assays of CCRF-CEM cells after incubation with FAM-Sgc8 (red line) and FAM-TD05 (green line, as the control probe), respectively. The flow cytometry assays were performed by counting 10 000 events, and the concentrations of both aptamers was 25 nM. (B) The confocal fluorescence (a, c) and transmission (b, d) images of CCRF-CEM cells incubated with GO/FAM-Sgc8 (a, b) and GO/FAM-TD05 (c, d), respectively. Scale bar: 10 μm, scan at 20× objective.

has no strong interaction with target CCRF-CEM cells and does not recover the quenched fluorescence of GO/FAM-TD05. Notably, when HeLa cells were incubated with GO/FAM-Sgc8 (or GO/FAM-TD05), no obvious fluorescence signal was recorded for these two mixture solutions (Fig. S3, ESI†), again suggesting that the high-specificity and high-affinity of the Sgc8 aptamer to target CCRF-CEM cells are the main reasons for selective fluorescence recovery of the GO/FAM-Sgc8. All these results provide a promising pathway for applying the GO-based FRET aptasensor in a microfluidic chip for the detection of CCRF-CEM cells.

An integrated microchip for high-throughput cell analysis

In order to establish the high-throughput assay for CCRF-CEM cells, we developed a microfluidic chip integrated with the GO-based FRET aptasensing strategy and detected with a confocal fluorescence scanning microscopy. As a proof of concept, 7 microchannels were pipetted with a 40 μL mixture of samples containing GO/FAM-Sgc8 and serial dilutions (10-fold) of CCRF-CEM cells ranging from 2.5×10^1 to 2.5×10^6 cells mL^{-1}. From the scanning image of the 7 microchannels (as shown in Fig. 5), a cell concentration-dependent change of fluorescent intensity was observed in such a multichannel chip, and the fluorescent intensity of GO/FAM-Sgc8 increased with the increasing concentration of CCRF-CEM cells. By plotting the fluorescent intensities (at 520 nm) *versus* the concentrations of cells, a linear range from 2.5×10^1 to 2.5×10^4 cells mL^{-1} was obtained, with a regression coefficient of 0.997 (Fig. 5C). The detection limit of this assay is 25 cells mL^{-1}, which is 7.2 times lower than that of the colorimetric aptasensor with gold nanoparticles,[12] and 23.6 times lower than that of the FRET aptasensor.[14] In such an integrated microfluidic chip, the improved performances for detecting CCRF-CEM cells can be ascribed to the high quenching efficiency of GO as a nanoquencher and the high affinity of Sgc8 aptamer towards CCRF-CEM (with a 0.80 nM of dissociation constants, K_d).[14] More importantly, compared with the conventional, single-sample assay, our microfluidic chip integrated with the GO-based FRET biosensor is simpler, faster and more efficient, which can simultaneously detect 7 different concentrations of CCRF-CEM cell samples (40 μL) in 30 min, and its efficiency of our integrated chip will be further improved when it comes to assay more samples.

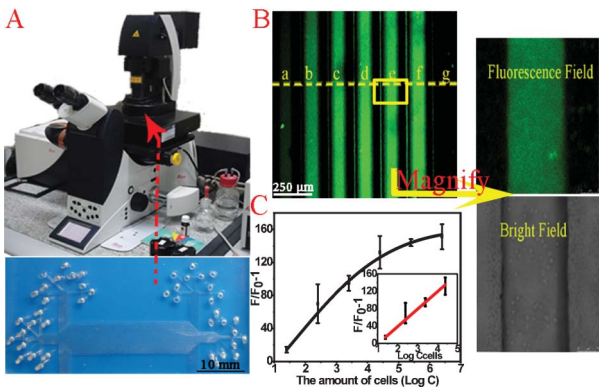

Fig. 5 The high-throughput PDMS-microfluidic chip integrated with the 'signal-on' GO/FAM-Sgc8 aptasensor for the detection of CCRF-CEM cells. (A) Photographs of the laser confocal microscopy with the multichannel microfluidic chip (the inset). (B) The fluorescence micrograph of the aptasensing microfluidic chip with different cell concentrations (from a–f: 2.5×10^1 to 2.5×10^6 cells mL^{-1}, g: the control) in each microchannel. The inserted bright and fluorescence field images of channel e were magnified and captured respectively. (C) The linear relationship between the fluorescence intensity of GO/FAM-Sgc8 and the amount of CCRF-CEM cells in microchannels. Excitation wavelength: 488 nm. Scale bar: 250 μm.

The selectivity of this microfluidic chip towards CCRF-CEM cells was evaluated by testing the response of the assay to other cell lines, including Raji cells, MCF-7 cells, HeLa cells, and NCIH1650 cells, at a concentration of 2.5×10^6 cells mL^{-1}. As shown in Fig. 6, fluorescent intensities of GO/FAM-Sgc8 in the integrated microfluidic chip negligibly changed with the additions of the control cells, while a significant fluorescence increase was observed for CCRF-CEM cells. The high selectivity of GO/FAM-Sgc8 is attributed to the high specificity of FAM-Sgc8 towards CCRF-CEM cells. Meanwhile, the relative standard deviation (RSD) of the recovered fluorescence for GO/FAM-Sgc8 toward the same CCRF-CEM cells (2.5×10^3 cells mL^{-1}) in 7 parallel microchannels of such a microfluidic chip was found to be 4.8%. Therefore, the microfluidic chip can be applied in the detection of CCRF-CEM cells with high specificity and acceptable reproducibility.

To make sure no cell harm was caused by using the GO-based aptasensing microfluidic chip, the cytotoxicity of the GO in the CCRF-CEM cells was investigated by using a CCK-8 cell viability assay. Fig. S4 (ESI†) shows the viability of the cells incubated with six different concentrations of GO. Even after an incubation of 24 h with 100 μg mL^{-1} GO, the cell viability remained greater than 86.0%. These viabilities were comparable to the controls, and these results indicate that the GO/FAM-Sgc8 is a harmless fluorescent probe and can be applied for long-term detection of living CCRF-CEM cells.

Conclusions

A multichannel microfluidic chip integrated with a novel GO-based FRET biosensor was created for the *in situ* detection of CCRF-CEM cells by assaying the cell-induced fluorescence recovery from the GO/FAM-Sgc8. The microfluidic chip has obvious advantages, *i.e.* 1) it realizes the on-chip analysis of CCRF-CEM cells with high-selectivity and high-sensitivity (at 25

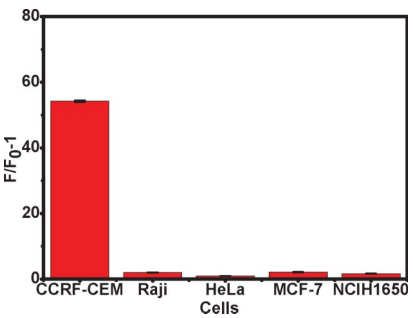

Fig. 6 Relative fluorescence intensity changes of the integrated microfluidic chip incubated with CCRF-CEM cells, Raji cells, HeLa cells, MCF-7 cells and NCIH1650 cells, respectively.

cells mL^{-1}), which is 10 times lower than those reported biosensors.[12,14] 2) it can quantitatively assay 7 different cell samples at same time by utilizing a parallel-scale homogenous detection. 3) it can visualize cancer cells in a 'signal-on' mode with a simplified FRET probe of GO/FAM-Sgc8. Given its easy operation, small volume, high sensitivity and high-throughput screening, this microfluidic assay is potentially useful for clinical cancer diagnosis and further treatment.

Acknowledgements

This work was supported by National Natural Science Foundation of China (21075021, 21175029 and 20890022) and the Shanghai Leading Academic Discipline Project (B109).

References

1 C. H. Dunphy, S. O. Orton and J. Mantell, *Am. J. Clin. Pathol.*, 2004, **122**, 865–874.
2 R. A. Ghossein and S. Bhattacharya, *Eur. J. Cancer*, 2000, **36**, 1681–1694.
3 V. Gubala, L. F. Harris, A. J. Ricco, M. X. Tan and D. E. Williams, *Anal. Chem.*, 2012, **84**, 487–515.
4 S. Nagrath, L. V. Sequist, S. Maheswaran, D. W. Bell, D. Irimia, L. Ulkus, M. R. Smith, E. L. Kwak, S. Digumarthy, A. Muzikansky, P. Ryan, U. J. Balis, R. G. Tompkins, D. A. Haber and M. Toner, *Nature*, 2007, **450**, 1235–1239.
5 Y. Xu, J. A. Phillips, J. L. Yan, Q. G. Li, Z. H. Fan and W. H. Tan, *Anal. Chem.*, 2009, **81**, 7436–7442.
6 K. Hoshino, Y.-Y. Huang, N. Lane, M. Huebschman, J. W. Uhr, E. P. Frenkel and X. Zhang, *Lab Chip*, 2011, **11**, 3449–3457.
7 J. Chen, J. Li and Y. Sun, *Lab Chip*, 2012, **12**, 1753–1767.
8 X. Zuo, S. Song, J. Zhang, D. Pan, L. Wang and C. Fan, *J. Am. Chem. Soc.*, 2007, **129**, 1042–1043.
9 B. R. Baker, R. Y. Lai, M. S. Wood, E. H. Doctor, A. J. Heeger and K. W. Plaxco, *J. Am. Chem. Soc.*, 2006, **128**, 3138–3139.
10 D. Shangguan, Z. Cao, L. Meng, P. Mallikaratchy, K. Sefah, H. Wang, Y. Li and W. Tan, *J. Proteome Res.*, 2008, **7**, 2133–2139.
11 C. D. Medley, S. Bamrungsap, W. Tan and J. E. Smith, *Anal. Chem.*, 2011, **83**, 727–734.
12 C. D. Medley, J. E.Smith, Z. Tang, Y. Wu, S. Bamrungsap and W. Tan, *Anal. Chem.*, 2008, **80**, 1067–1072.
13 D. H. Shangguan, L. Meng, Z. H. C. Cao, Z. Y. Xiao, X. H. Fang, Y. Li, D. Cardona, R. P. Witek, C. Liu and W. H. Tan, *Anal. Chem.*, 2008, **80**, 721–728.
14 H. Shi, X. He, K. Wang, X. Wu, X. Ye, Q. Guo, W. Tan, Z. Qing, X. Yang and B. Zhou, *Proc. Natl. Acad. Sci. U. S. A.*, 2011, **108**, 3900–3905.
15 F. Abachi and S. K. Noureini, *Clin. Biochem.*, 2011, **44**, S257–S257.
16 Y. He, M. Lu, J. Cao and H. P. Lu, *ACS Nano*, 2012, **6**, 1221–1229.
17 T. Sabir, G. F. Schroeder, A. Toulmin, P. McGlynn and S. W. Magennis, *J. Am. Chem. Soc.*, 2011, **133**, 1188–1191.
18 S. S. Varghese, Y. Zhu, T. J. Davis and S. C. Trowell, *Lab Chip*, 2010, **10**, 1355–1364.
19 F. Feng, L. Liu and S. Wang, *Nat. Protoc.*, 2010, **5**, 1255–1264.
20 Q. Zeng, Y. Zhang, X. Liu, L. Tu, X. Kong and H. Zhang, *Chem. Commun.*, 2012, **48**, 1781–1783.
21 S. J. Zhen, L. Q. Chen, S. J. Xiao, Y. F. Li, P. P. Hu, L. Zhan, L. Peng, E. Q. Song and C. Z. Huang, *Anal. Chem.*, 2010, **82**, 8432–8437.
22 S. J. He, B. Song, D. Li, C. F. Zhu, W. P. Qi, Y. Q. Wen, L. H. Wang, S. P. Song, H. P. Fang and C. H. Fan, *Adv. Funct. Mater.*, 2010, **20**, 453–459.
23 Y. Wang, Z. H. Li, D. H. Hu, C. T. Lin, J. H. Li and Y. H. Lin, *J. Am. Chem. Soc.*, 2010, **132**, 9274–9276.
24 C. Gomez-Navarro, R. T. Weitz, A. M. Bittner, M. Scolari, A. Mews, M. Burghard and K. Kern, *Nano Lett.*, 2007, **7**, 3499–3503.
25 X. M. Sun, Z. Liu, K. Welsher, J. T. Robinson, A. Goodwin, S. Zaric and H. J. Dai, *Nano Res.*, 2008, **1**, 203–212.
26 R. S. Swathi and K. L. Sebastian, *J. Chem. Phys.*, 2009, **130**, 086101.
27 C. H. Lu, H. H. Yang, C. L. Zhu, X. Chen and G. N. Chen, *Angew. Chem., Int. Ed.*, 2009, **48**, 4785–4787.
28 Y. He, Y. Lin, H. W. Tang and D. W. Pang, *Nanoscale*, 2012, **4**, 2054–2059.
29 H. X. Chang, L. H. Tang, Y. Wang, J. H. Jiang and J. H. Li, *Anal. Chem.*, 2010, **82**, 2341–2346.
30 X. Fang, H. Chen, L. Xu, X. Jiang, W. Wu and J. Kong, *Lab Chip*, 2012, **12**, 1495–1499.
31 J. Ji, Y. Zhao, L. Guo, B. Liu, C. Ji and P. Yang, *Lab Chip*, 2012, **12**, 1373–1377.
32 W. S. Hummers and R. E. Offeman, *J. Am. Chem. Soc.*, 1958, **20**, 1339.